Cytotoxic Effects of Green Synthesis Se/ZnO Nanoparticles on *Allium cepa* and their Potential to Inhibit Mycotoxin Synthesis

Abeer S. Meganid,^a Samy Selim,^{b,*} Mohamed A. Amin,^{c,*} Mahmoud Ezzat,^c Atyaf E. Dahlan,^d Mohammed S. Almuhayawi,^e Soad K. Al Jaouni,^f and Sulaiman A. Alsalamah,^g

Despite their dubious safety, nanoparticles (NPs) are beneficial in many areas, particularly in agriculture. Though a variety of commercial nanofertilizers, pesticides, and insecticides are available, little is known about their potential detrimental effects on plant cells. A Se/ZnO nanoparticle complex was synthesized utilizing Ficus nitida fruit extract as both a reducing and stabilizing agent, yielding an eco-friendly product. The common food plant Allium cepa was treated with Se/ZnO NP suspension. Transmission electron microscopic analyses of the NPs were performed, including Dynamic Light Scattering (DLS), zeta potential, X-ray diffraction, and FTIR characterizations. This study examined the cytological impact and chromosomal patterns of Allium cepa root meristems after treatment by Se/ZnO-NPs. Results show that all applied concentrations of NPs decreased the mitotic index (MI). The many chromosomal defects that were caused by NPs included disrupted and sticky chromosomes. Aflatoxin levels (B1, B2, G1, G2) were quantified in vegetables inoculated with Asperaillus flavus. Tomatoes and potatoes showed the highest contamination, in contrast, garlic and beet exhibited minimal or undetectable levels, suggesting resistance. The effect of Se/ZnO-NPs (0 to 40 ppm) on A. flavus growth and aflatoxin production was evaluated. While 5 ppm stimulated growth, higher concentrations significantly reduced both biomass and aflatoxins. These findings suggest that Se/ZnO- NPs treatment as an effective strategy to suppress A. flavus and its toxin production in contaminated crops.

DOI: 10.15376/biores.20.4.10170-10187

Keywords: Allium cepa; Root tips; Nanoparticles; Fungi; Ficus nitida; Mycotoxins; Chromosomes

Contact information: a: College of Science and Humanities- Jubail, Imam Abdulrahman Bin Faisal University, Jubail, Saudi Arabia; b: Department of Clinical Laboratory Sciences, College of Applied Medical Sciences, Jouf University, Sakaka 72388, Saudi Arabia; c: Botany and Microbiology Department, Faculty of Science (Boys), Al-Azhar University, Cairo 11884, Egypt; d: Pharmacy Department, Jazan University Hospital, Jazan, Saudi Arabia; e: Department of Clinical Microbiology and Immunology, College of Medicine, King Abdulaziz University, Jeddah 21589, Saudi Arabia; f: Department of Hematology/Oncology, Scientific Chair of Prophetic Medicine Application, College of Medicine, King Abdulaziz University, Jeddah 21589, Saudi Arabia; g: Department of Biology, College of Science, Imam Mohammad Ibn Saud Islamic University (IMSIU), Riyadh 11623, Saudi Arabia;

* Corresponding author: sabdulsalam@ju.edu.sa (S.S.); mamin7780@azhar.edu.eg (M. A.A.)

INTRODUCTION

Nanoparticles (NPs) can change the physicochemical processes of different substances, which can have a significant biological impact on cells (Atallah and Yassin 2020). It is challenging to predict their beneficial or detrimental impacts and their modes of action in biological systems and the environment because of the diverse sizes and forms of these entities (Chen et al. 2020). The biological technique provides a relatively safe alternative to the other methods used to synthesize NPs, even though cytotoxicity, genotoxicity, and oxidative stress are the main ways that NPs cause harm. The synthesis of plant and microbial extracts has garnered significant attention as an eco-friendly and sustainable method for producing a range of NPs (Karimi and Mahdavi Shahri 2021). The development and application of nanotechnology have impacted multiple domains, involving drugs and food production. Understanding the advantages and disadvantages of these products is essential for ensuring their sustainable and optimal use (Selim et al. 2025a; Amin et al. 2024, 2025). Nonetheless, the heightened prevalence of Se or ZnO nanoparticles (NPs) in commercial items has elicited escalating public apprehension their toxicological and environmental ramifications. Toxicological investigations conducted in the past decade have revealed that ZnO NPs pose possible health and environmental concerns, but there have been no studies related to Se/ZnO NPs and their effects on plant cells, especially the mitotic index and abnormalities of cell phases. The ZnO NPs exhibit significant toxicity to bacteria, freshwater microalgae, mice, and human cells (Hou et al. 2018). Abdelsalam et al. (2022) observed that 150 ppm of amino-Zn NPs after 24 h, appeared to decrease the mitotic index by 35.3% on Triticum aestivum L compared to the control, which was 88.0%. In a study conducted on Lens culinaris Medik., the mitotic index in root tip cells decreased at all concentrations of ZnO-NPs treatment (25 and 50 ppm) in comparison to the control. Especially, the mitotic index was at its lowest point at the maximum concentration (50 ppm) (Dogan 2024).

Vegetables are highly perishable commodities, and their high moisture content makes them particularly susceptible to fungal contamination during postharvest handling, transportation, and storage (El-Taher et al. 2012; Abdelghany and Bakri 2019; Al-Rajhi et al. 2023a). Fungal species such as Penicillium, Aspergillus, and Fusarium are commonly associated with vegetable spoilage, causing visible decay, softening, discoloration, and unpleasant odors (Abdelghany 2014). These fungi typically invade through wounds, cracks, or damaged tissues and thrive under humid and warm conditions. In addition to physical spoilage, their presence reduces the nutritional and commercial value of vegetables, leading to significant economic losses. Among the various fungi associated with vegetable spoilage, Aspergillus flavus is of particular concern due to its ability to produce aflatoxins, which are highly toxic and carcinogenic secondary metabolites. Aflatoxins, particularly B1, B2, G1, and G2, pose a major threat to food safety and public health (Hamed et al. 2016). They can contaminate a wide range of agricultural products, including nuts, grains, spices, and, under favorable conditions, vegetables. Poor storage conditions, mechanical damage, and high humidity increase the risk of aflatoxin contamination in vegetable crops, especially in warm climates (Abd El-Ghany 2006; Mariutti and Valente 2009; Abdel-Kader et al. 2025). The consumption of aflatoxincontaminated vegetables may result in serious health issues such as liver damage, immune suppression, and, with chronic exposure, liver cancer (Nuhu et al. 2025). Regulatory authorities have set strict maximum limits for aflatoxins in food products to protect consumers. Therefore, identifying fungal contaminants and monitoring aflatoxin levels in vegetables is crucial for ensuring food safety. Preventive strategies include improving postharvest handling, proper drying and storage, and the use of antifungal treatments or biocontrol agents to minimize fungal growth and toxin production (Abdel Ghany 2014; Al-Rajhi *et al.* 2022, 2023b). It is hypothesized that some metal ions can be released in a controlled manner *via* nanoparticles. Ion exchange with the solid material is made possible by the nanomaterial's extremely high surface area, which results from its extremely small size. Compared to liquid soil supplements, the solid structure of the nanoparticles makes them less prone to leaching into groundwater. This study succeeded in creating Se/ZnO NPs based on underutilized *Ficus nitida* fruit extract, and also aimed to examine the effects of Se/ZnO NPs on chromosomal aberrations, mitotic index of the economic plant *Allium cepa* L., as well as on fungal growth and its mycotoxins.

EXPERIMENTAL

Extraction of Ficus nitida Fruits

The fruits of *Ficus nitida* (common name: curtain fig) were obtained from the Street garden at Sakaka city, Aljouf Region (Saudi Arabia). *Ficus* fruits contain many active compounds, such as phenolic compounds, fatty acids, and sugars. Such compounds may act as stabilizers, capping agents, or reducing agents, thereby facilitating the preparation of NPs. The most common bioactive substances present in many species are phenolic acids, which include caffeic, chlorogenic, and gallic acids (dos Anjos Cruz et al., 2022).

The fruits were crushed after being cleaned with water that was distilled and let to air dry for two weeks. 5 g of air-dried powder and 100 mL of distilled water were combined, and the combination was sonicated for two hours at 50 °C in a water bath to create the fruit aqueous extract. The filtrate was kept in a refrigerator at 4 °C after the extract was filtered through filter paper (Whatman No. 1).

Synthesis of Selenium/ Zinc Oxide Nanoparticles based on *Ficus nitida* Fruit Extract

A magnetic stirrer was used to mix 30 mL of the aqueous fruit extract in a 250 mL flask to produce Se/ZnO nanoparticles. The flask was then filled with ten milliliters of sodium selenite (1 mM) and zinc nitrate (1 mM). The mixture was agitated for 48 h at 250 °C. The reaction mixture's color change indicated the formation of Se/ZnO NPs. The nanospheres were precipitated using centrifugation for 20 minutes at 4 °C and 14,000 rpm. The pellets were thoroughly cleaned in deionized water before freeze-drying (Selim et al. 2025b).

Characterization of Se/ZnO NPs

Utilizing an X-ray diffractometer (D8-Advance; Bruker, Germany), the microstructure of the nanomaterial was evaluated. The Scherer equation, $D=0.9\,\lambda/\beta\cos\theta$, was used to measure the particle size of NPs. Then the *d*-spacing ($d_{hkl}=\lambda/(2\sin\theta)$) values (Table 1). A transmission electron microscope (HR-TEM, JEOL-JEM-2100) was used to assess the generated NPs' size and shape. Using Fourier transform infrared spectroscopy, the functional groups connected to the produced NPs was analyzed. A Malvern Zetasizer

2000 (Nano-ZS; Malvern Instruments, Malvern, UK) with dynamic light scattering (DLS) was used to measure the mean size and zeta potential of Se/ZnO NPs suspended in deionized water at 25 °C.

Cytological Studies

Different concentrations of Se/ZnO NPs (5, 10, and 20 ppm) were produced as solutions in deionized water. The vitality of the seedlings was assessed after 6, 12, and 24 hours of the seeds sprouting in a small bottle containing varying concentrations of Se/ZnO NPs. Following treatment, the seeds were removed from the treatment device and rinsed with deionized water. To facilitate cytological processing, the tops of the roots were carefully cut. The root tips of the research plants were used for cytological processing after careful extraction. Using freshly made Carnoy's fixative (3:1 v/v absolute alcohol and glacial acetic acid, respectively), the root tips of both treated and untreated plants were fixed. The tips ranged in length from 1 to 2 cm. Feulgen squash was used to create cytological slides (Darlington and La Cour 1976). To confirm and count the chromosomal anomalies, the slides were examined under a microscope and photographed using an XSZ-N 107 research microscope equipped with a Premiere MA88-900 digital camera.

Fungal Isolation and Identification

To remove outside contaminants without compromising internal fungal structures, small pieces of spoiled vegetables (potato, garlic, beet, tomato, eggplant, onion, carrot, cucumber, broccoli, and pepper) were removed from areas that were obviously decomposed and surface-sterilized for 2 min using 1% sodium hypochlorite. After sterilizing, these segments were placed on potato dextrose agar (PDA) plates and incubated at 30°C to encourage the growth of fungi. The same incubation conditions were used to subculture newly formed fungal colonies in order to guarantee culture purity. Morphological and microscopic criteria were used to identify the dominant isolated fungus. The identification process followed the taxonomic keys and descriptions provided by Samson *et al.* (1995).

Industrial Infection of Vegetables with *Aspergillus flavus* for Mycotoxin Production

A toxigenic strain of A. flavus (previously isolated and confirmed for aflatoxin production) was cultured on potato dextrose agar (PDA) plates and incubated at 28 ± 2 °C for 7 days. Conidia were harvested by adding sterile 0.1% of polysorbate 80 (Tween 80) solution to the plate and gently scraping the surface. The spore suspension was filtered through sterile muslin cloth and adjusted to a concentration of 1×10^6 spores/mL using a hemocytometer. Ten types of fresh vegetables, such as potato, garlic, beet, tomato, eggplant, onion, carrot, cucumber, broccoli, and pepper were selected based on their economic relevance and susceptibility to fungal contamination. Vegetables were washed under running tap water, surface sterilized with 1% sodium hypochlorite for 2 min, and rinsed three times with sterile distilled water. Each vegetable was wounded at 2 to 3 sites (approx. 5 mm depth) using a sterile scalpel. A 50 μ L aliquot of the A. flavus spore suspension was pipetted into each wound site. Control samples were treated with sterile polysorbate 80 solution without spores. Inoculated vegetables were placed individually in sterile plastic containers lined with moist filter paper to maintain high humidity ($\geq 90\%$). Incubation was conducted at 28 ± 2 °C for 15 days under dark conditions to mimic storage

environments conducive to aflatoxin production (Dijksterhuis and Houbraken 2025). After the incubation period, visibly infected tissue from each vegetable was excised, homogenized, and subjected to mycotoxin extraction. Aflatoxins were extracted using a mixture of methanol: water (80:20, v/v). Quantification of aflatoxins (B1, B2, G1, and G2) was performed using an ELISA kit. The aflatoxin concentrations were expressed in $\mu g/kg$ of fresh weight.

Effect of Bimetallic Se/ZnO NPs on Growth and Mycotoxin Production by Aspergillus flavus

The following experimental protocol was used to assess the impact of bimetallic Se/ZnO NPs on the growth and production of aflatoxin by *A. flavus*: A toxigenic strain of *A. flavus* was cultivated and kept on PDA slants at 4°C. Se/ZnO NPs were suspended in sterile distilled water and sonicated to ensure even dispersion. Five concentrations (0, 5, 10, 20, and 40 ppm) were prepared and aseptically added to 100 mL of sterilized PDB in 250 mL Erlenmeyer flasks. Each flask was inoculated with 1 mL of a freshly made spore suspension from A. flavus (1 × 10⁶ spores/mL). The flasks were incubated at 28 °C under stationary conditions for 10 days. After incubation, the fungal biomass was harvested by filtration through pre-weighed Whatman No. 1 filter paper, washed with sterile distilled water, and dried at 60 °C to constant weight. The biomass was expressed as mg/100 mL of culture medium (Al-Rajhi *et al.* 2022). The culture filtrates were collected and subjected to liquid-liquid extraction for aflatoxin determination.

Mycotoxins Assay

Mycotoxin analysis was conducted using a microtiter plate enzyme-linked immunosorbent assay (ELISA) with an automated Chem-well reader and commercial test kits for Aspergillus and Fusarium mycotoxins (R-Biopharm). The assay targeted aflatoxins B1, B2, G1, G2, and zearalenone, following the manufacturer's protocol (Al-Rajhi et al. 2024). For sample preparation, 10 mL of homogenized fungal broth was mixed with 20 mL of 70% methanol and stirred for 10 min using a magnetic stirrer. The mixture was then filtered through Whatman No. 1 filter paper. A volume of 5 mL of the filtrate was diluted with 15 mL of distilled water and 0.25 mL of polysorbate 20, followed by 2 min of mixing using a magnetic stirrer. For the ELISA procedure, 50 µL of each standard toxin solution (5, 10, 20, 45 ppb) and $50 \mu\text{L}$ of the prepared sample extract were added to individual wells of the microtiter plate. Plates were incubated at room temperature. After incubation, the wells were emptied and washed three times with 250 μL of PBS-polysorbate buffer (pH 7.2). Subsequently, 50 µL of enzyme conjugate and 50 µL of the chromogenic substrate tetramethylbenzidine (TMB) were added to each well and incubated in the dark at room temperature for 30 min (Hamed et al. 2016). The reaction was stopped by adding 100 µL of 1 M H₂SO₄, and absorbance was measured at 450 nm using the ELISA reader.

Analytical Statistics

Minitab 18 was utilized for statistical computations at the probability level of 0.05. Analyses of variance, one-way ANOVA, and post hoc Tukey's test were employed to examine quantitative data with a parametric distribution.

RESULTS AND DISCUSSION

Characterization of Se/ZnO NPs

A complex of Se/ZnO NPs was created using *Ficus nitida* fruit extract as a reducing and stabilizing agent, resulting in an environmentally friendly product. Zinc oxide NPs were combined with selenium (Se) to yield Se/ZnO NPs. The inclusion of Se may improve electrical properties, surface characteristics, and overall efficiency (Song *et al.* 2022). The nanoparticle manufacturing process demonstrated a notable color change to a dark brown hue. This visually confirmed the formation of Se/ZnO NPs (Mirzaei *et al.* 2021).

TEM and DLS analysis (Figs. 1A, 1C) are critical for assessing the shape, dimensions, distribution, and surface area of the synthesized Se/ZnO NPs. The TEM images obtained demonstrate that the NPs had semispherical and irregular shapes (Fig. 1A). The particle size was determined to be 48.8 nm, as measured by DLS analysis (Fig. 1C). The FTIR spectrum (Fig. 1B) reveals the vibrations and expanding peaks associated with functional groups that share in NPs formation. In the NPs solution, eight significant peaks were observed at 3415, 2919, 1602, 1413, 1348, 1118, 615, and 509 cm⁻¹. The presence of various functional groups in fruit extract, such as hydroxyl, carbonyl group, facilitated the reduction, capping, and stabilization of Se/ZnO NPs (Nguyen et al. 2023). The vibrations caused by stretching of O-H (alcohols and phenols) are located at 3415 cm⁻¹ (Demir et al. 2018). The stretching vibration of the carboxyl group C=O accounts for the absorbance band at 1348 cm⁻¹. The ZnO bond was recognized as the origin of a significant vibration band at 615 cm⁻¹ (El-Badri et al. 2021). At 509 cm⁻¹, the presence of selenium metal was observed (Jyoti et al. 2016). Figure 1D illustrates the investigation of the zeta potential of the synthesized Se/ZnO NPs at the synthesis pH of 7.2. The synthesized NPs exhibited a consistently negative surface zeta potential at the pH level analyzed in this study. The zeta potential of the preparation at a neutral pH of 7.2 was measured at -33.0 mV, as shown in Fig. 1D.

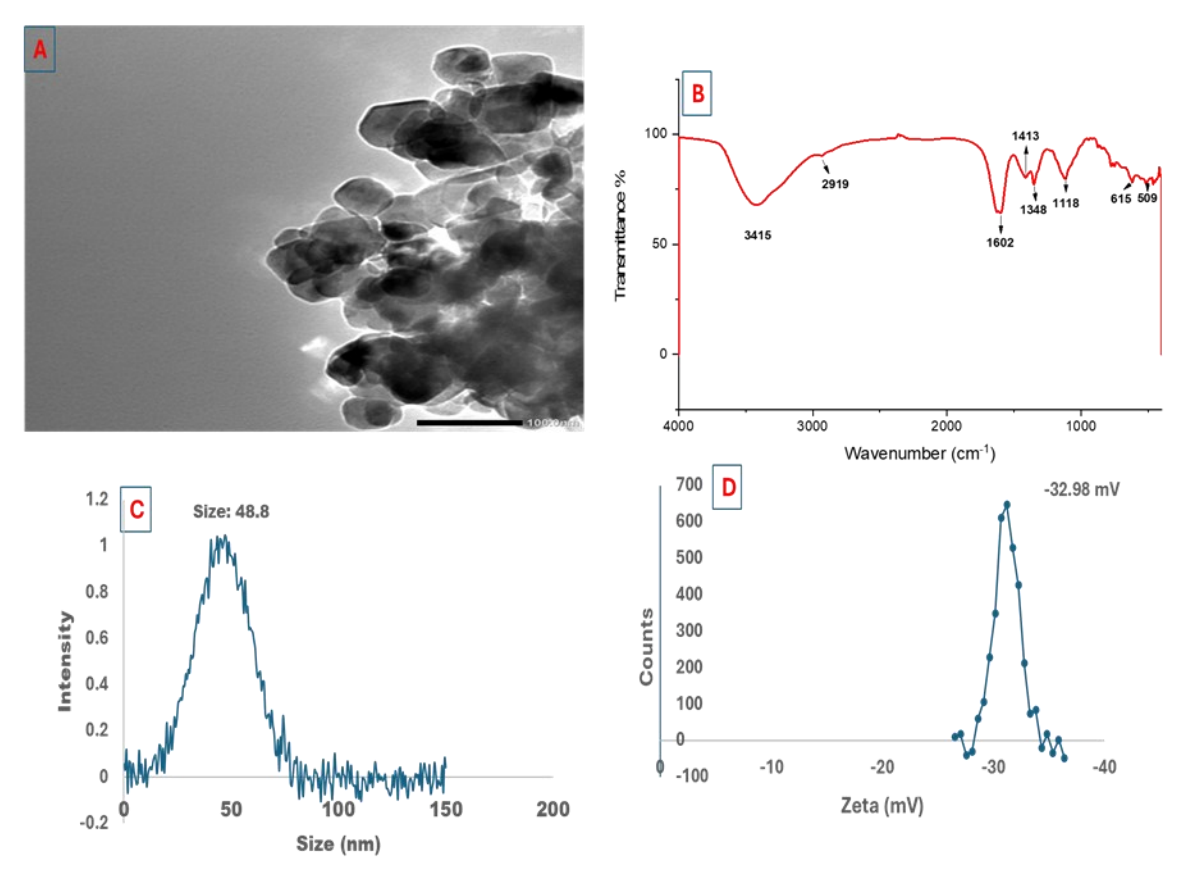


Fig. 1. TEM image (A), FTIR (B), DLS analysis (C), and Zeta potential (D) of Se/ZnO NPs

XRD Analysis

One useful method for determining the crystal structure of NPs is the XRD spectrum. The XRD diffraction spectra of the produced Se/ZnO NPs are shown in Fig. 2, where a clear and noticeable Bragg reflection was present.

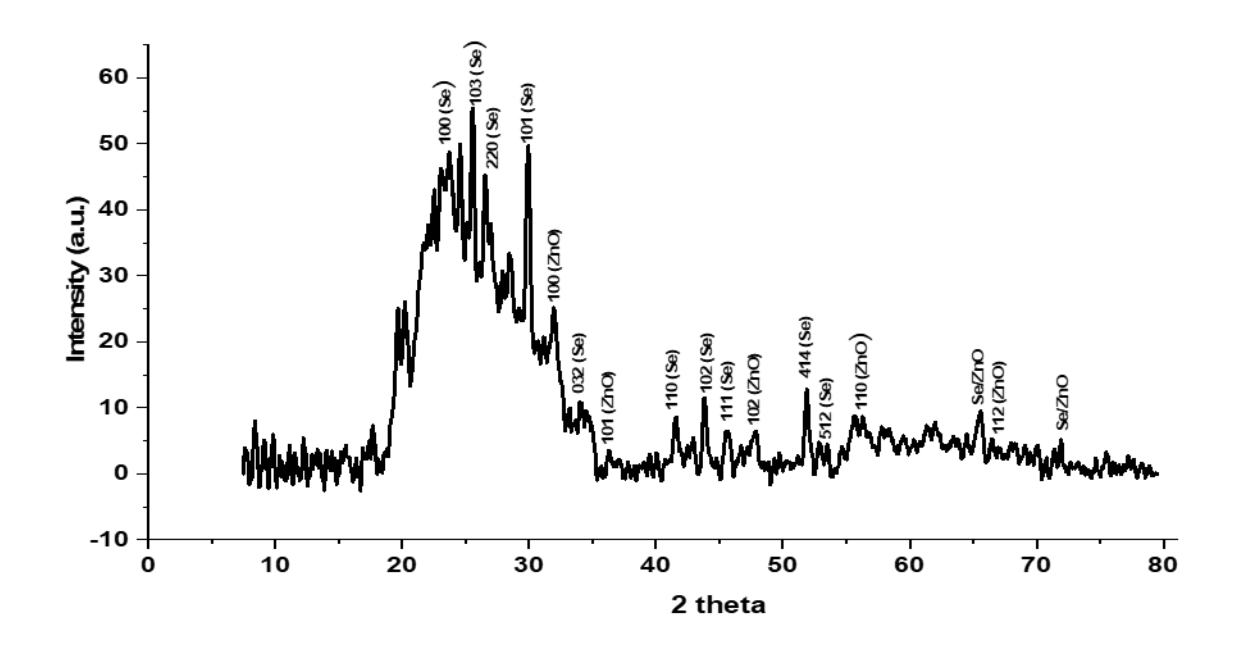


Fig. 2. XRD analysis of the Se/ZnO NPs

Table 1. XRD Parameters for Se/ZnO NPs

2θ (°)	FWHM (β)	Size (nm)	<i>d</i> -spacing
23.46	5.77	1.405	1.93
25.61	6.79	1.199	1.78
27.19	7.22	1.131	1.68
29.93	1.32	6.229	1.54
31.97	0.99	8.336	1.45
33.56	1.13	7.339	1.39
36.69	1.32	6.340	1.28
41.58	1.36	6.437	1.16
43.84	0.37	22.96	1.11
45.63	0.46	18.52	1.07
47.59	1.07	8.071	1.04
51.88	0.87	10.15	0.97
53.54	0.65	13.68	0.95
56.43	7.35	1.225	0.92
68.32	0.87	11.03	0.82
Average	0.62	8.27	1.27

The XRD's sharp peaks demonstrated the crystalline nature of the NPs generated. According to the hkl miller indices, the peaks at 23.4°, 25.6°, 27.2, 29.9°, 33.5°, 41.5°, 43.8°, 45.6°, 51.8°, and 53.5° respectively correspond to crystal planes 100, 103, 220, 101, 032, 110, 102, 111, 414, and 512 crystalline Se (COD9008579, 9008581, and JCPDS card No. 06–362) (El-Batal *et al.* 2023) is indicated by these peaks. Another group of 2θ was visible in the XRD spectrum in Fig. 2 at 31.9°, 36.6°, 47.5°, 56.4°, and 68.3°. Accordingly, these angles corresponded to the Miller indices of 100, 101, 102, 110, and 112. Crystalline ZnO (COD 2107059, 1011259, and JCPDS 5-0664) is represented by these peaks. Se/ZnO NPs (average = 8.27 nm) had particle sizes that were slightly smaller than the TEM measurement, according to the Scherer equation. The amorphous peaks were

seen in the XRD pattern. According to Indhira *et al.* (2023), Se-ZnO NPs must be heated to roughly 400 °C to achieve a crystalline form. It can degrade the bioactive metabolites in the specimen and stop biological activity at this temperature point. This implies that the NPs are crystalline and that *Ficus nitida* fruit extract is a stabilizing agent. XRD parameters for Se/ZnO NPs are shown in Table 1.

Genotoxic Effects of Se/ZnO NPs

The potential phytotoxic and genotoxic impacts of Se/ZnO Nanocomposite on garlic (Tables 2 and 3, and Figs. 3 and 4) were examined. The Se/ZnO NPs inhibited mitosis index in a concentration-dependent manner and created several mitotic abnormalities, including chromosomal stickiness, irregular prophase, disturbed metaphase, C-metaphase, and bridges. Higher concentrations of ZnO NPs were found to exacerbate chromosomal aberrations and reduce the mitotic index (Raskar and Laware, 2014). Table 2 illustrates how Se/ZnO NPs affect the mitotic index (MI). According to the findings, the Se/ZnO NPs caused the root tip cells of Allium cepa to undergo mitodepression. Nevertheless, in comparison to lower concentrations and control cells, larger concentrations of nanoparticles had a noticeably bigger effect on the MI value. The reduction observed was substantial across all treatments for NPs, with a particularly remarkable significance noted in the treatment involving 20 ppm Se/ZnO NP over a 24-h duration, where the MI was measured at 1.80±0.096, in comparison to the control group's MI of 5.11±0.044.

Zinc ions are responsible for the reduction in the rate of mitotic division because they impede the transition of cells from the S (DNA synthesis) phase to the M (mitosis) phase. Exposure to ZnO has the effect of preventing many cells from progressing to prophase and interfering with the mitotic cycle. The decrease in the MI value can be used to gauge the degree of cytotoxicity (Ramesh et al. 2014). The findings indicated an elevated frequency of prophase and metaphase stages at the expense of other mitotic phases in Se/ZnO NPs. The accumulation observed during these stages suggests that zinc ions play a significant role in modulating the sequence of mitotic division, effectively diminishing the number of cells that proceed to mitotic division by obstructing the process after prophase. Table 3 presents the percentages of chromosomal abnormalities attributed to NPs. The percentage of abnormalities reached 100% following treatment with 20 ppm for 24-h. The abnormal percentage was 42.4% following treatment with 5 ppm for 6-h, in contrast to 16.5% observed in control cells. Table 3 indicates that NPs elicited various types of mitotic abnormal cells in the root tip of *Allium cepa* seeds. Several of these types are illustrated in Fig. 3. The proportion of these types varied with the concentration and duration of treatment. These categories encompassed sticky at various stages, irregular prophase, and C-C-metaphase. During prophase, a high frequency of irregular prophase and sticky prophase was observed. The frequency of irregular prophase was elevated during shorter treatment durations, whereas sticky prophase was more prevalent at the longest treatment duration. The irregular formation of prophase is influenced by the effects of Se and Zn ions on the individualization of chromatin threads into normal. ZnO NPs' genotoxicity and biochemical effects on Vicia faba, Nicotiana tabacum, and Allium cepa plants were assessed by Ghosh et al. (2016). According to their findings, Allium cepa cells' root meristems displayed higher chromosome abnormalities, cell-cycle, micronucleus production, and membrane integrity loss.

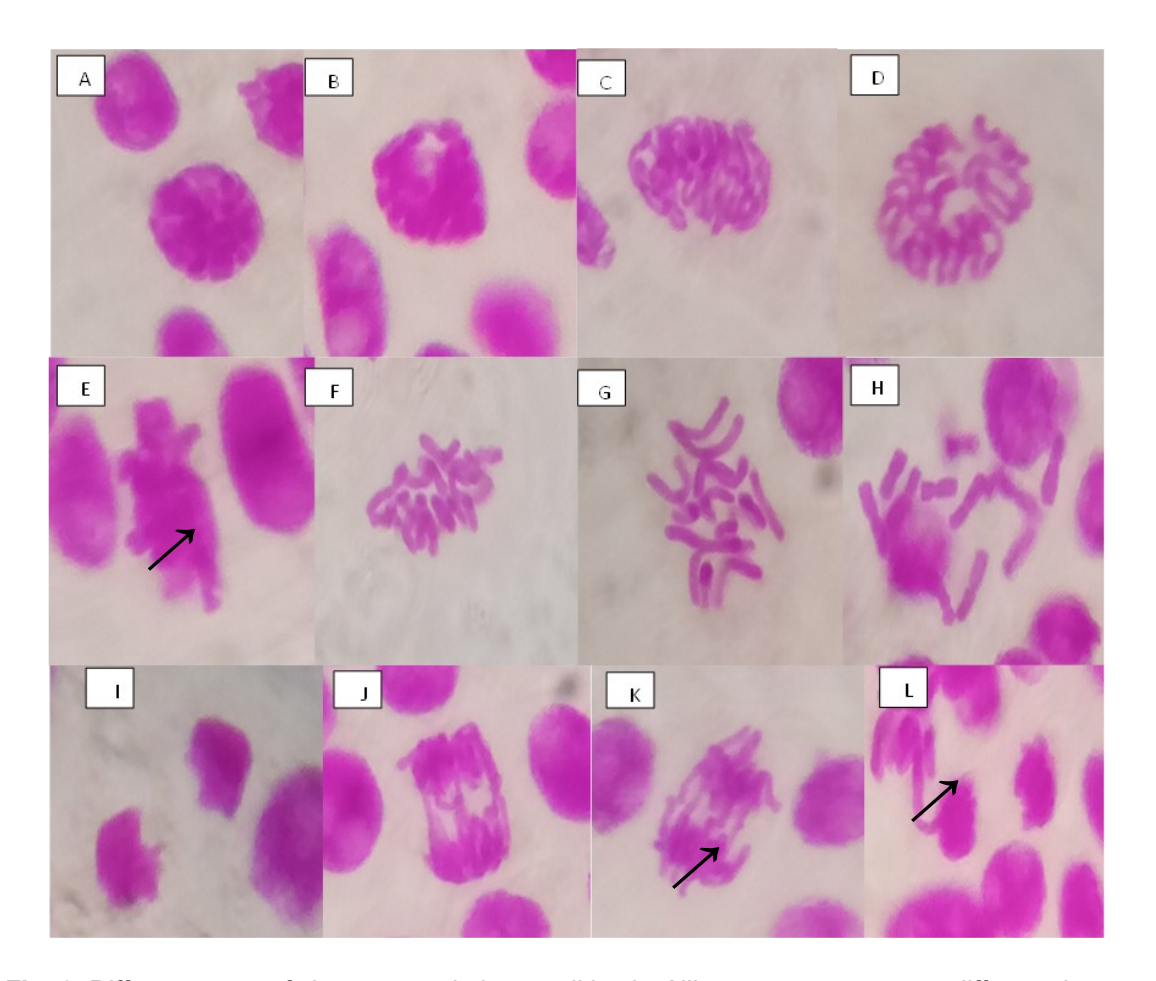


Fig. 3. Different types of chromosomal abnormalities in *Allium cepa* response to different times and concentrations of biogenic bimetallic Se/ZnO NPs: (A) Sticky prophase, (B) sticky vacuolated nucleus at prophase, (C, D) irregular prophase, (E) sticky metaphase, (F) disturbed metaphase, (G, H) C- metaphase, (I) Sticky anaphase, (J) sticky anaphase with multi-bridges, (K) sticky anaphase with multi-bridges and forward chromosomes, and (L) sticky telophase with forward chromosome.

5228

94

Treatn	nents	Counted Cells	Divided Cells	Mitotic Index	Mitotic Phases (%)			
Conc.	Time			(MI ± S.E)				
(ppm)	(h)				Prophase	Metaphase	Anaphase	Telophase
Con	trol	5345	273	5.11±0.044	50	28.88	5.56	15.55
	6	5599	257	4.59±0.103	46.15	38.46	0.00	15.38
5ppm	12	5089	192	3.77±0.085	38.98	40.68	3.39	16.95
	24	5215	148	2.84±0.022	43.14	39.22	3.92	13.73
10	6	5486	205	3.74±0.118	37.14	30.00	14.29	18.57
ppm	12	5275	150	2.84±0.135	39.22	23.53	15.69	21.57
	24	5417	135	2.49±0.105	33.33	26.19	19.05	21.43
20	6	5693	156	2.74±0.063	28.85	40.38	17.31	13.46
ppm	12	5401	114	2.11±0.108	30.30	30.30	18.18	21.21

Table 2. Types and Percentages of Mitotic Abnormal and Total Abnormal Cells in *Allium cepa* Root Tips Treated with Se/ZnO NPs at Different Times

Table 3. Types and Percentages of Mitotic Abnormal and Total Abnormal Cells in *Allium cepa* Root Tips Treated with Se/ZnO NPs at Different Times and Concentrations

31.03

27.59

20.69

20.69

1.80±0.096

Treatmo	ents	Divided Cells	Total Abnormal	Ab. (%)	Abnormal Mitotic Phases (%)		6)	
Conc.	Time		Cells					
(ppm)	(h)				Prophase	Metaphase	Anaphase	Telophase
Contr	ol	273	45	16.48±0.81	6.59	5.13	1.83	2.93
	6	257	109	42.41±0.91	16.34	15.56	2.33	8.17
5 ppm	12	192	110	57.29±0.53	20.31	19.79	2.60	14.58
	24	148	108	72.97±1.05	23.65	31.08	4.05	14.19
10 ppm	6	205	141	68.78±0.97	17.56	22.93	14.63	13.66
	12	150	123	82.00±0.98	28.67	21.33	15.33	16.67
	24	135	125	92.59±0.50	26.67	25.19	19.26	21.48
20 ppm	6	156	138	88.46±1.50	23.08	35.90	17.31	12.18
	12	114	110	96.49±0.83	30.70	27.19	17.54	21.05
	24	94	94	100±0.00	31.91	27.66	20.21	20.21

Types of Aflatoxins - Aflatoxins B1, B2, G1, and G2-detected in Various Vegetables

A comprehensive analysis of the levels of four types of aflatoxins- Aflatoxin B1, B2, G1, and G2-detected in various vegetables artificially infected with *A. flavus* is shown in Table 4. Among the vegetables tested, tomatoes, potatoes, and peppers recorded the highest levels of aflatoxins across all types. Specifically, tomatoes showed the highest concentration of Aflatoxin B1 ($4.50 \pm 0.01~\mu g/kg$) and significant levels of B2, G1, and G2, suggesting that they are highly susceptible to contamination. Potatoes followed closely with $4.33 \pm 0.06~\mu g/kg$ of Aflatoxin B1 and high levels of B2 ($1.95 \pm 0.01~\mu g/kg$), G1 ($1.10 \pm 0.18~\mu g/kg$), and G2 ($0.40 \pm 0.04~\mu g/kg$). Peppers also exhibited substantial contamination, particularly with Aflatoxin B2 ($1.76 \pm 0.02~\mu g/kg$) and G2 ($0.58 \pm 0.04~\mu g/kg$). In contrast, garlic and beet exhibited no detectable levels of Aflatoxin G1 and G2 ($0.00 \pm 0.00~\mu g/kg$), which may indicate either resistance to *A. flavus* growth or its inability to produce them in those substrates. Garlic, in particular, had low levels of B1 and B2 ($1.77 \pm 0.06~and~0.31 \pm 0.01~\mu g/kg$, respectively), while beet showed slightly higher but still moderate levels of B1 and B2. Onions also demonstrated relatively low aflatoxin levels, particularly for B1 ($1.53 \pm 0.18~\mu g/kg$), but detectable levels of G1 and G2 (0.58 ± 0.04

and $0.61 \pm 0.02 \,\mu \text{g/kg}$), suggesting selective susceptibility. Vegetables such as broccoli, eggplants, cucumbers, and carrots showed intermediate contamination levels, indicating that while not as heavily affected as tomatoes or potatoes, they are still vulnerable to mycotoxin accumulation under favorable conditions for fungal growth. The statistical differences among vegetable types were supported by the Least Significant Difference (LSD) values, which were 0.43, 0.22, 0.10, and 0.15 µg/kg for Aflatoxins B1, B2, G1, and G2, respectively. These relatively low thresholds, particularly for G1 and G2, mean that even small variations in toxin levels are statistically meaningful. Generally, the data clearly showed that the susceptibility of vegetables to aflatoxin contamination by A. flavus varied significantly. Tomatoes and potatoes pose the highest risk, which is likely due to their high moisture content and soft tissue structure, which favor fungal colonization and toxin production. In contrast, garlic, beet, and to some extent onions appear to be more resistant, potentially due to their antimicrobial compounds or less favorable internal environments for fungal growth. These results underscore the importance of targeted postharvest handling, storage, and food safety monitoring, especially for the more vulnerable vegetables in the context of mycotoxin contamination.

Van de Perre et al. (2014) reported the presence of several fungi and different mycotoxins on various vegetables including tomatoes, soft red fruits, onions, and bell peppers. Capsicum and its derivative products are highly susceptible to contamination by mycotoxins, particularly during postharvest handling and storage under inadequate conditions. This vulnerability underscores the importance of developing effective antifungal strategies to minimize fungal growth and mycotoxin biosynthesis (Costa et al. 2019). Our results were agreeing with other studies, where the presence of A. flavus in fresh fruit of tomato has been reported (Segura-Palacios et al. 2021). While previous study, Maroutti (2009) informed the documentation of the fungi namely A. flavus and A. parasiticus besides the occurrence of aflatoxins in fresh tomato fruit as well as by-products including ketchup, pulp, paste, dried tomatoes preserved in oil and dehydrated tomatoes. Ali et al. (2024) revealed fungal contamination of onions by Aspergillus niger, Fusarium species, and Rhizopus stolonifer. Notably, A. niger isolated from the infected onion samples demonstrated the ability to produce ochratoxin A (Esuola and Ortega-Beltran 2025), highlighting its potential risk as a foodborne toxigenic pathogen.

Table 4. Mycotoxin Detection in Different Vegetables Infected with by A. flavus

Vegetables	Aflatoxin B1 (μg/kg)	Aflatoxin B2 (μg/kg)	Aflatoxin G1 (μg/kg)	Aflatoxin G2 (µg/kg)
Garlic	1.77±0.06d	0.31±0.01d	0.00±0.0	0.00±0.00
Broccoli	2.40±0.04c	0.49±0.04d	0.29±0.01e	0.19±0.01d
Peppers	3.88±0.12b	1.76±0.02ab	1.47±0.24a	0.58±0.04b
Eggplants	2.65±0.04c	0.78±0.01c	0.56±0.02cd	0.31±0.02c
Beet	2.99±0.07c	0.71±0.04c	0.40±0.01d	0.00±0.00
Onions	1.53±0.18d	0.87±0.03c	0.58±0.04c	0.61±0.02b
Potatoes	4.33±0.06a	1.95±0.01a	1.50±0.18a	0.89±0.05a
Tomatoes	4.50±0.01a	1.56±0.04b	0.78±0.07b	0.48±0.01b
Cucumbers	3.50±0.05b	0.88±0.01c	0.61±0.06c	0.23±0.03c
Carrots	2.66±0.01c	0.78±0.02c	0.66±0.01c	0.34±0.02c
LSD	0.43	0.22	0.10	0.15

The results in Table 5 demonstrate the impact of various doses (ranging from 0 to 40 ppm) of bimetallic Se/ZnO NPs on the growth and Aflatoxins (B1, B2, G1, and G2) production of A. flavus. A. flavus showed a baseline growth of 255 ± 2.12 mg and produced considerable amounts of all four aflatoxins, with Aflatoxin B1 at $6.54 \pm 0.32 \,\mu g/kg$, B2 at $3.68 \pm 0.18 \,\mu \text{g/kg}$, G1 at $2.42 \pm 0.10 \,\mu \text{g/kg}$, and G2 at $1.77 \pm 0.01 \,\mu \text{g/kg}$ at 0 ppm (the control) of Se/ZnO NPs. Interestingly, when treated with a low concentration of 5 ppm Se/ZnO NPs, A. flavus growth significantly increased to 320 ± 3.23 mg. This unexpected stimulation may reflect a hormetic effect, where sublethal stress enhances biological activity, or it could result from trace element uptake stimulating fungal metabolism at low doses. However, with increasing nanoparticle concentrations, a gradual decline in A. flavus growth was evident. At 10 ppm, growth dropped to 278 ± 4.32 mg, and further reductions were seen at 20 ppm (223 \pm 1.36 mg) and 40 ppm (168 \pm 1.65 mg). This downward trend clearly suggests that higher doses of Se/ZnO NPs exert an inhibitory effect on A. flavus biomass, likely due to oxidative stress, cell wall damage, or Se/ZnO NPs interaction with vital cellular processes. Aflatoxin production followed a similar pattern. At 5 ppm, despite the increased A. flavus biomass, aflatoxin levels remained high, with AFB1 and B2 even exceeding control levels slightly. However, as Se/ZnO NPs concentrations increased, aflatoxin production decreased markedly. At 10 ppm, AFB1 dropped to $6.22 \pm 0.25 \mu g/kg$ and continued decreasing to $2.66 \pm 0.36 \,\mu\text{g/kg}$ at 20 ppm and $2.54 \pm 0.26 \,\mu\text{g/kg}$ at 40 ppm. The same trend was observed with AFB2, AFG1, and AFG2, all of which were sharply reduced. Of particular note is Aflatoxin G2, which was completely undetectable at 40 ppm, suggesting a complete inhibition of its biosynthetic pathway under these conditions. The values of LSD provided—12.36 for A. flavus growth, 0.32 for AFB1, 0.54 for AFB2, 0.62 for AFG1, and 0.24 for AFG2—support the statistical significance of these changes. Previously, numerous investigations employed NPs of silver for controlling aflatoxins (Abdelghany et al. 2020) and other mycotoxins (Bakri et al. 2020; Al-Rajhi et al. 2022). According to Hassan et al. (2013), growth of fungi and its productivity of aflatoxins were suppressed via the addition of ZnO-NPs at 8 µg/mL, whereas the growth of ochratoxin Aand fumonisin B1-producing fungi, along with their mycotoxin production, was suppressed by incorporating 10 µg/mL of ZnO-NPs into the tested medium. Also, recent study demonstrated the ability of ZnO-CuO NPs to inhibit aflatoxin production in maize (Ngwenya et al. 2025).

Table 5. Effect of Se/ZnO NPs on Growth and Mycotoxin Production by A. flavus

Conc (ppm)	Growth mg/100 mL	Aflatoxin Quantity					
(ррііі)	medium	Aflatoxin B1	Aflatoxin B2	Aflatoxin G1	Aflatoxin G2		
0	255±2.12c	6.54±0.32b	3.68±0.18b	2.42±0.10b	1.77±0.01a		
5	320±3.23a	7.59±0.15a	5.87±0.21a	3.92±0.06a	1.89±0.02a		
10	278±4.32b	6.22±0.25b	3.12±0.08c	2.11±0.04b	1.58±0.06b		
20	223±1.36d	2.66±0.36c	1.56±0.03d	0.86±0.09c	0.21±0.03c		
40	168±1.65e	2.54±0.26c	1.12±0.04d	0.34±0.02c	0.0±0.00		
LSD	12.36	0.32	0.54	0.62	0.24		

CONCLUSIONS

- 1. Se/ZnO nanoparticles (NPs) exhibited a concentration-dependent dual effect on *Aspergillus flavus*, initially stimulating growth at very low levels but progressively suppressing both growth and mycotoxin production as the concentration increases.
- 2. The results highlight the potential of Se/ZnO NPs as an effective antifungal and antimycotoxigenic agent, particularly at higher concentrations (20 to 40 ppm).
- 3. Evidence was found of genetic disruption in *A. flavus* exposed to the Se/ZnO NPs, which raises concerns about possible unintended effects. Such risks, in addition to reports from previous studies on nanoparticle toxicity and environmental persistence, underline the importance of caution.
- 4. Therefore, while Se/ZnO NPs demonstrate promise for nanoparticle-based control strategies in food preservation and fungal contamination prevention, their potential risks must be carefully weighed. Further investigation is necessary to fully assess their safety, genetic impact, and compatibility with food and agricultural systems before large-scale application.

FUNDING

This work was funded by the Deanship of Graduate Studies and Scientific Research at Jouf University under grant No. (DGSSR-2025-FC-01007).

REFERENCES CITED

- Abd El-Ghany, T. M. (2006). "Metabolic regulation of fungal reproduction and their secondary metabolites," *Al-Azhar Bull. Sci.* 17(1), 87-102. DOI: 10.21608/absb.2006.14728
- Abdelghany, T. M. (2014). "Eco-friendly role of *Juniperus procera* as safe alternative for controlling fungal growth and their secondary metabolites," *The African Journal of Mycology and Biotechnology* 19(1), 21-36.
- Abdelghany, T. M., and Bakri, M. M. (2019). "Effectiveness of a biological agent (*Trichoderma harzianum* and its culture filtrate) and a fungicide (methyl benzimacold-2-ylcarbamate) on the tomato rotting activity (growth, cellulolytic, and pectinolytic activities) of *Alternaria solani*," *BioResources* 14(1), 1591-1602. DOI: 10.15376/biores.14.1.1591-1602
- Abdelghany, T. M., Hassan, M. M., El-Naggar, M. A., and Abd El-Mongy, M. (2020). "GC/MS analysis of *Juniperus procera* extract and its activity with silver nanoparticles against *Aspergillus flavus* growth and aflatoxins production," *Biotechnology Reports* 27, article e00496. DOI: 10.1016/j.btre.2020.e00496.
- Abdel-Kader, M. M., Ibrahim, M. I. M., Khalil, M. S. A., El-Mougy, N. S., and El-Gamal, N. G. (2025). "Pre-storage treatments for suppressing of aflatoxins production in wheat grains," *Cereal Research Communications* 53, 903-912. DOI: 10.1007/s42976-024-00560-0.

- Abdelsalam, N. R., Abdel-Megeed, A., Ghareeb, R. Y., Ali, H. M., Salem, M. Z., Akrami, M., Al-Hayalif, M. F. A., and Desoky, E. S. M. (2022). "Genotoxicity assessment of amino zinc nanoparticles in wheat (*Triticum aestivum* L.) as cytogenetical perspective," *Saudi Journal of Biological Sciences* 29(4), 2306-2313. DOI: 10.1016/j.sjbs.2021.11.059.
- Ali, S. M., AbdulAali, R. M., Alshimaysawe, U. A. A. A. A., and Ali, A. M. (2024). "Isolation and identification of fungi contaminating onion bulbs, detection of *Aspergillus* spp. toxins, and inhibiting its growth by *Moringa oleifera* extract," *Kufa Journal for Agricultural Sciences* 16(2), 104-113. DOI: 10.36077/kjas/2024/v16i2.16108.
- Al-Rajhi, A. M. H., Yahya, R., Alawlaqi, M. M., Fareid, M. A., Amin, B. H., and Abdelghany, T. M. (2022). "Copper oxide nanoparticles as fungistat to inhibit mycotoxins and hydrolytic enzyme production by *Fusarium incarnatum* isolated from garlic biomass," *BioResources* 17(2), 3042-3056. DOI: 10.15376/biores.17.2.3042-3056.
- Al-Rajhi, A. M., Moawad, H., Alawlaqi, M. M., Felemban, H. R., and Abdelghany, T. M. (2023a). "Bread spoilage fungi as creators of α-amylase using two types of wheat flour," *BioResources* 18(3), 5908-5923. DOI: 10.15376/biores.18.3.5908-5923.
- Al-Rajhi, A. M., Salem, O. M., Mohammad, A. M., and Ghany, T. M. (2023b). "Mycotoxins associated with maize wastes treated with comprised capsule of *Spirulina platensis* biomass," *BioResources* 18(3), 4532-4542. DOI: 10.15376/biores.18.3.4532-4542.
- Al-Rajhi, A. M., Ganash, M., Alshammari, A. N., Alsalamah, S. A., and Abdelghany, T. M. (2024). "*In vitro* and molecular docking evaluation of target proteins of lipase and protease for the degradation of aflatoxins," *BioResources* 19(2), 2701-2713. DOI: 10.15376/biores.19.2.2701-2713
- Amin, M. A. A., Abu-Elsaoud, A. M., Nowwar, A. I., Abdelwahab, A. T., Awad, M. A., Hassan, S. E. D., and Elkelish, A. (2024). "Green synthesis of magnesium oxide nanoparticles using endophytic fungal strain to improve the growth, metabolic activities, yield traits, and phenolic compounds content of *Nigella sativa L.*," *Green Processing and Synthesis* 13(1), 20230215. DOI: 10.1515/gps-2023-0215.
- Amin, M. A., Algamdi, N. A., Waznah, M. S., Bukhari, D. A., Alsharif, S. M., Alkhayri, F., Abdel-Nasser, M., and Fouda, A. (2025). "An insight into antimicrobial, antioxidant, anticancer, and antidiabetic activities of trimetallic Se/ZnO/CuO nanoalloys fabricated by aqueous extract of *Nitraria retusa*," *Journal of Cluster Science* 36(1), 1-15. DOI: 10.1007/s10876-024-02742-6.
- Atallah, O., and Yassin, S. (2020). "Aspergillus spp. eliminate Sclerotinia sclerotiorum by imbalancing the ambient oxalic acid concentration and parasitizing its sclerotia," Environmental Microbiology 22(12), 5265-5279.
- Bakri, M. M., Al-Rajhi, A. M. H., Abada, E., Salem, O. M. A., Shater, A.-R., Mahmoud, M. S., and Abdel Ghany, T. M. (2022). "Mycostimulator of chitinolytic activity: Thermodynamic studies and its activity against human and food-borne microbial pathogens," *BioResources* 17(3), 4378-4394. DOI: 10.15376/biores.17.3.4378-4394.
- Chen, Z., Yu, G., and Wang, Q. (2020). "Effects of climate and forest age on the ecosystem carbon exchange of afforestation," *Journal of Forestry Research* 31(2), 365-374. DOI: 10.1007/s11676-019-00946-5.

- Costa, J., Rodríguez, R., Garcia-Cela, E., Medina, A., Magan, N., Lima, N., Battilani, P., and Santos, C. (2019). "Overview of fungi and mycotoxin contamination in *Capsicum* pepper and in its derivatives," *Toxins* 11(1), article 27. DOI: 10.3390/toxins11010027.
- Darlington, C.D., and La Cour, L. F. (1976). *The Handling of Chromosomes*, 6th edn, Wiley, New York.
- Demir, D., Bölgen, N., and Vaseashta, A. (2018). "Green synthesis of silver nanoparticles using *Lantana camara* leaf extract and their use as mercury (II) ion sensor," in: *Advanced Nanotechnologies for Detection and Defence against CBRN Agents*, Springer, Dordrecht, pp. 427-433. DOI: 10.1007/978-94-024-1298-7 42
- Dijksterhuis, J., and Houbraken, J. (2025). "Fungal spoilage of crops and food," in: S. Grüttner, K. Kollath-Leiß, and F. Kempken (eds.), *Agricultural and Industrial Applications. The Mycota*, Vol. 16. Springer, Cham. DOI: 10.1007/978-3-031-81904-9 3
- Dogan, G. (2024). "Genotoxic and cytotoxic effects of zinc oxide nanoparticles (ZnO-NPs) synthesized by hydrothermal method on lentils (*Lens culinaris* Medik.)," *Cytologia* 89(4), 285-295. DOI: 10.1508/cytologia.89.285.
- Dos Anjos Cruz, J. M., Corrêa, R. F., Lamarão, C. V., Kinupp, V. F., Sanches, E. A., Campelo, P. H., and de Araújo Bezerra, J. (2022). "Ficus spp. fruits: Bioactive compounds and chemical, biological and pharmacological properties," Food Research International 152, article 110928. DOI:10.1016/j.foodres.2021.110928
- El-Badri, A. M. A., Batool, M., Mohamed, I. A. A., Khatab, A., Sherif, A., Wang, Z., Salah, A., Nishawy, E., Ayaad, M., Kuai, J., Wang, B., and Zhou, G. (2021). "Modulation of salinity impact on early seedling stage *via* nano-priming application of zinc oxide on rapeseed (*Brassica napus* L.)," *Plant Physiology and Biochemistry* 166, 376-392. DOI: 10.1016/j.ecoenv.2021.112695.
- El-Batal, A. I., Ismail, M. A., Amin, M. A., El-Sayyad, G. S., and Osman, M. S. (2023). "Selenium nanoparticles induce growth and physiological tolerance of wastewater stressed carrot plants," *Biologia* 78(9), 2339-2355. DOI:10.1007/s11756-023-01401-x.
- El-Taher, E. M., Abel-Ghany, T. M., Alawlaqi, M. M., and Ashour, M. S. (2012). "Biosecurity for reducing ochratoxin A productivity and their impact on germination and ultrastructures of germinated wheat grains," *Journal of Microbiology, Biotechnology and Food Science* 2(1), 135-151.
- Esuola, C. O., and Ortega-Beltran, A. (2025). "Fumonisin and ochratoxin-producing strains of *Aspergillus* section Nigri are associated with onion (*Allium cepa* L.) bulbs sold in markets in southwest Nigeria," *Frontiers in Fungal Biology* 6, article 1563824. DOI: 10.3389/ffunb.2025.1563824
- Ghosh, M., Jana, A., Sinha, S., Jothiramajayam, M., Nag, A., Chakraborty, A., and Mukherjee, A. (2016). "Effects of ZnO nanoparticles in plants: Cytotoxicity, genotoxicity, deregulation of antioxidant defenses, and cell-cycle arrest," *Mutation Research/Genetic Toxicology and Environmental Mutagenesis* 807, 25-32.
- Hamed, M. A., Abdel Ghany, T. M., Elhussieny, N. I., and Nabih, M. A. (2016). "Exploration of fungal infection in agricultural grains, aflatoxin and zearalenone synthesis under pH stress," *International Journal of Current Microbiology and Applied Sciences* 5(4), 1007-1017. DOI: 10.20546/ijcmas.2016.504.115
- Hassan, A. A., Howayda, M. E., and Mahmoud, H. H. (2013). "Effect of zinc oxide nanoparticles on the growth of mycotoxigenic mould," *Studies in Chemical Process Technology* 1(4).

- Hou, J., Wu, Y., Li, X., Wei, B., Li, S., and Wang, X. (2018). "Toxic effects of different types of zinc oxide nanoparticles on algae, plants, invertebrates, vertebrates and microorganisms," *Chemosphere* 193, 852-860. DOI: 10.1016/j.chemosphere.2017.11.077
- Indhira, D., Aruna, A., Manikandan, K., Albeshr, M. F., Alrefaei, A. F., Vinayagam, R., Kathirvel, A., Priyan, S. R., Kumar, G. S., and Srinivasan, R. (2023). "Antimicrobial and photocatalytic activities of selenium nanoparticles synthesized from *Elaeagnus indica* leaf extract," *Processes* 11(4), article no. 1107. DOI: 10.3390/pr11041107
- Jyoti, K., Baunthiyal, M., and Singh, A. (2016). "Characterization of silver nanoparticles synthesized using *Urtica dioica* Linn. leaves and their synergistic effects with antibiotics," *Journal of Radiation Research and Applied Sciences* 9(3), 217-227. DOI: 10.1016/j.jrras.2015.10.002
- Karimi, S., and Mahdavi Shahri, M. (2021). "Medical and cytotoxicity effects of green synthesized silver nanoparticles using *Achillea millefolium* extract on MOLT-4 lymphoblastic leukemia cell line," *Journal of Medical Virology* 93(6), 3899-3906. DOI: 10.1002/jmv.26694
- Mariutti, L. R., and Valente, L. M. (2009). "Survey of aflatoxins in tomato products," *Ciência e Tecnologia de Alimentos* 29, 431-434. DOI: 10.1590/S0101-20612009000200031
- Mirzaei, S. Z., Somaghian, S. A., Lashgarian, H. E., Karkhane, M., Cheraghipour, K., and Marzban, A. (2021). "Phyco-fabrication of bimetallic nanoparticles (zinc–selenium) using aqueous extract of *Gracilaria corticata* and its biological activity potentials," *Ceramics International* 47(4), 5580-5586. DOI: 10.1016/j.ceramint.2020.10.142
- Nguyen, T. T. T., Nguyen, Y. N. N., Tran, X. T., Nguyen, T. T. T., and Van Tran, T. (2023). "Green synthesis of CuO, ZnO and CuO/ZnO nanoparticles using *Annona glabra* leaf extract for antioxidant, antibacterial and photocatalytic activities," *Journal of Environmental Chemical Engineering* 11(5), article no. 111003. DOI: 10.1016/j.jece.2023.111003
- Ngwenya, S. C., Sithole, N. J., Mthiyane, D. M. N., Jobe, M. C., Babalola, O. O., Ayangbenro, A. S., Mwanza, M., Onwudiwe, D. C., and Ramachela, K. (2025). "Effects of green-synthesised copper oxide–zinc oxide hybrid nanoparticles on antifungal activity and phytotoxicity of aflatoxin B1 in maize (*Zea mays* L.) seed germination," *Agronomy* 15(2), article 313. DOI: 10.3390/agronomy15020313
- Nuhu, A. H., Dorleku, W. P., Blay, B., Derban, E., McArthur, C. O., Alobuia, S. E., Incoom, A., Dontoh, D., Ofosu, I. W., and Oduro-Mensah, D. (2025). "Exposure to aflatoxins and ochratoxin A from the consumption of selected staples and fresh cow milk in the wet and dry seasons in Ghana," *Food Control* 168, article 110968. DOI: 10.1016/j.foodcont.2024.110968
- Ramesh, M., Palanisamy, K., Babu, K., and Sharma, N. K. (2014). "Effects of bulk and nano-titanium dioxide and zinc oxide on physio-morphological changes in *Triticum aestivum* Linn.," *Journal of Global Biosciences* 3(2), 415-422.
- Raskar, S. V., and Laware, S. L. (2014). "Effect of zinc oxide nanoparticles on cytology and seed germination in onion," *International Journal of Current Microbiology and Applied Sciences* 3(2), 467-473.
- Samson, R. A., Hoekstra, E. S., Frisvad, J. C., and Filtenborg, O. (1995). *Introduction to Food-Borne Fungi* (4th Ed.), Centraalbureau voor Schimmelcultures (CBS), Baarn, The Netherlands, 322 pp.

- Segura-Palacios, M. A., Correa-Pacheco, Z. N., Corona-Rangel, M. L., Martinez-Ramirez, O. C., Salazar-Piña, D. A., Ramos-García, M. L., and Bautista-Baños, S. (2021). "Use of natural products on the control of *Aspergillus flavus* and production of aflatoxins *in vitro* and on tomato fruit," *Plants* 10(12), article 2553. DOI: 10.3390/plants10122553
- Selim, S., Almuhayawi, M. S., Alruhaili, M. H., Tarabulsi, M. K., Saddiq, A. A., Elamir, M. Y. M., Amin, M. A., and Al Jaouni, S. K. (2025a). "Pharmacological applications and plant stimulation under sea water stress of biosynthesis bimetallic ZnO/MgO NPs," *Scientific Reports* 15(1), article 5263. DOI: 10.1038/s41598-025-87881-0
- Selim, S., Saddiq, A. A., Ashy, R. A., Baghdadi, A. M., Alzahrani, A. J., Mostafa, E. M., Al Jaouni, S. K., Elamir, M. Y. M., Amin, M. A., Salah, A. M., *et al.* (2025b). "Bimetallic selenium/zinc oxide nanoparticles: Biological activity and plant biostimulant properties," *AMB Express* 15(1), 1-11. DOI: 10.1186/s13568-024-01808-y
- Song, Y., Yang, F., Ma, M., Kang, Y., Hui, A., Quan, Z., and Wang, A. (2022). "Green synthesized Se–ZnO/attapulgite nanocomposites using *Aloe vera* leaf extract: Characterization, antibacterial and antioxidant activities," *LWT* 165, article 113762. DOI: 10.1016/j.lwt.2022.113762
- Van de Perre, E., Deschuyffeleer, N., Jacxsens, L., Vekeman, F., Van Der Hauwaert, W., Asam, S., and De Meulenaer, B. (2014). "Screening of moulds and mycotoxins in tomatoes, bell peppers, onions, soft red fruits and derived tomato products," *Food Control* 37, 165-170. DOI: 10.1016/j.foodcont.2013.09.034

Article submitted: September 12, 2025; Peer review completed: October 1,2025; Revised version received and accepted: October 2, 2025; Published: October 10, 2025. DOI: 10.15376/biores.20.4.10170-10187